Cellular Signalling 28 (2016) 561–571

Contents lists available at ScienceDirect

Cellular Signalling

journal homepage: www.elsevier.com/locate/cellsig

Regulation of BRAF protein stability by a negative feedback loop involving the MEK–ERK pathway but not the FBXW7 tumour suppressor

Maria Aguilar Hernandez [a,1], Bipin Patel [a], Fiona Hey [a], Susan Giblett [a], Hayley Davis [c], Catrin Pritchard [a,b,*]

[a] Department of Molecular Cell Biology, University of Leicester, University Road, Leicester LE1 7RH, UK
[b] Department of Cancer Studies, University of Leicester, University Road, Leicester LE1 7RH, UK
[c] Gastrointestinal Stem Cell Biology Laboratory, Wellcome Trust Centre for Human Genetics, Oxford University, Roosevelt Drive, Oxford OX3 7BN, UK

ARTICLE INFO

Article history:
Received 12 November 2015
Received in revised form 8 February 2016
Accepted 15 February 2016
Available online 17 February 2016

Keywords:
BRAF
ERK
Feedback
FBXW7
Protein stability

ABSTRACT

The ^{V600E}*BRAF* oncogenic mutation is detected in a wide range of human cancers and induces hyperactivation of the downstream MEK–ERK signalling cascade. Although output of the BRAF–MEK–ERK pathway is regulated by feed-forward RAF activity, feedback control also plays an important role. One such feedback pathway has been identified in *Caenorhabditis elegans* and involves ERK-mediated phosphorylation of BRAF within a CDC4 phosphodegron (CPD), targeting BRAF for degradation *via* CDC4 (also known as FBXW7), a component of the SKP1/CUL1/F-box (SCF) E3 ubiquitin ligase complex. Here we investigate this pathway in mammalian cells. Short-term expression of autochthonous ^{V600E}BRAF in mouse embryonic fibroblasts (MEFs) leads to down-regulation of BRAF protein levels in a proteasome-dependent manner and ^{V600E}BRAF has a reduced half-life compared to ^{WT}BRAF in HEK293^{T} cells. These effects were reversed by treatment with the MEK inhibitor PD184352. We have identified the equivalent CPD at residues 400–405 in human BRAF and have found that mutation of ERK phosphorylation sites at residues T401 and S405 in ^{V600E}BRAF increases the half-life of the protein. While BRAF and FBXW7 co-immunoprecipitated, the overexpression of FBXW7 did not influence the half-life of either ^{WT}BRAF or ^{V600E}BRAF. Furthermore, disruption of the substrate-binding site of mouse FBXW7 using the R482Q mutation did not affect the interaction with BRAF and the expression levels of ^{WT}BRAF and ^{V600E}BRAF were not altered in MEFs derived from mice with the homozygous knockin ^{R482Q}*FBXW7* mutation. Overall these data confirm the existence of a negative feedback pathway by which BRAF protein stability is regulated by ERK. However, unlike the situation in *C. elegans*, FBXW7 does not play a unique role in mediating subsequent BRAF degradation.

1. Introduction

The BRAF protein kinase is a key component of the RAF–MEK–ERK signalling cascade. This pathway plays a major role in controlling numerous cellular events including cell proliferation, survival, differentiation and migration [1,2]. Tight regulation of the pathway is vital for normal cell, tissue and whole body homeostasis. This is evidenced by the fact that hyperactive, oncogenic forms of *BRAF* are prevalent in several human cancers [3]. The ^{V600E}*BRAF* mutation is the most common *BRAF* mutation detected in human cancers and is thought to mediate its transforming effects by deregulation of the MEK–ERK pathway [4–6]. Loss of function mutations in components of the pathway such as BRAF also give rise to embryonic lethality with a failure to thrive associated with placental failure [7,8].

The mechanisms of regulation of the ERK pathway have been subjected to extensive investigation with evidence showing that the pathway can be controlled by feed-forward and feedback loops [9–11]. Regulatory loops fall into immediate and late temporal domains. The immediate responses include protein–protein interactions such as dimerization [12–14] and covalent protein modifications particularly cycles of phosphorylation and dephosphorylation [15–17], both of which influence RAF activation/deactivation and subsequent downstream signalling. Late events involve newly synthesised proteins, for example the induction of expression of adapters SPROUTYs and SPREDS [18–20] as well as phosphatases [21–23] that have been shown to suppress ERK pathway activity through feedback mechanisms. The activity of feedback control pathways is important in cancer development as evidenced by the fact that disabled feedback inhibitory pathways are detected in ^{V600E}BRAF transformed cells [24], while clinical and

Abbreviations: C. elegans, *Caenorhabditis elegans*; MEK, mitogen-activated protein kinase kinase; ERK, extracellular signal-regulated kinase; CPD, CDC4 phosphodegron; DMEM, Dulbecco's modified Eagle's medium; DMSO, dimethylsulphoxide; MEFs, mouse embryonic fibroblasts; AdCre, adenoviral-Cre; GLB, gold lysis buffer; GFP, green fluorescent protein; SCF, SKP1/CUL1/F-box.

* Corresponding author at: Department of Cancer Studies, University of Leicester, University Road, Leicester Le1 7RH, UK.
E-mail address: cap8@le.ac.uk (C. Pritchard).
[1] Present address: Instituto Nacional de Pediatria, Insurgentes Sur 3700-C, Col. Insurgentes, Cuicuilco, C.P. 04530, México, D.F.

http://dx.doi.org/10.1016/j.cellsig.2016.02.009

experimental evidence is consistent with most negative regulators of the ERK pathway being tumour suppressors [25].

Regulation of protein stability is an important factor in controlling signalling pathway output. An example of this is for the EGF receptor whereby ligand-induced autophosphorylation allows recruitment of the CBL E3 ubiquitin ligase, which controls EGFR internalisation and degradation [26,27]. With regard to RAF, the correct folding and stabilisation of the proteins is dependent on the molecular chaperone HSP90 complex [28] and pharmacological inhibition of HSP90 leads to their ubiquitin-mediated degradation, particularly for ^{V600E}BRAF which shows a greater dependence on HSP90 than ^{WT}BRAF, CRAF or ARAF [29,30]. A study using siRNA has shown a requirement for the E3 ubiquitin ligase Cullin-5 in mediating ^{V600E}BRAF degradation following HSP90 inhibition [31]. The Ring finger protein 149 (RNF149) has also been proposed to be an E3 ubiquitin ligase active operating on the kinase domain of ^{WT}BRAF [32] while a further study in *Caenorhabditis elegans* identified that the BRAF homologue, LIN-45, is a substrate for the multiprotein E3 ubiquitin ligase Skp1/Cul1/F-box (SCF) complex [33]. The F-box containing substrate receptor SEL-10 (FBXW7 in mammals) was shown to target LIN-45 through a conserved Cdc4 phosphodegron (CPD) and, additionally, the ERK homologue MPK-1 was found to be required for controlling LIN-45 degradation through the CPD in a negative feedback loop [33].

Here, we have investigated BRAF protein turnover in mammalian cells. Using MEFs derived from mice bearing a conditional knockin allele for ^{V600E}BRAF [34] we show that expression of ^{V600E}BRAF leads to downregulation of BRAF protein expression. This downregulation is not associated with alterations in *Braf* mRNA levels, but can be rescued by proteasome and MEK inhibition. Ectopically expressed V600EBRAF also has a shorter half-life by ~3 h than ^{WT}BRAF and this can be rescued by MEK inhibition. A conserved CPD at residues 400–405 in human BRAF was identified and we show that the feedback regulation can in part be explained by ERK-mediated phosphorylation of T401 and S405 since mutation of these residues increases the half-life of ^{V600E}BRAF. However, although BRAF has the capability to bind to FBXW7, FBXW7 over-expression or loss of function does not alter either ^{WT}BRAF or ^{V600E}BRAF protein stability, suggesting that this E3 ubiquitin ligase component is not uniquely involved in regulating mammalian BRAF turnover. We also demonstrate an association between this novel feedback pathway and the oncogene-induced senescence phenotype.

2. Materials and methods

2.1. Animal work

Braf$^{+/LSL\text{-}V600E}$ mice have been described previously [34] and the induction of lung tumour development by intercrossing with the CreER™ strain [35] has been reported in [36]. The conditional knockin *Fbxw7*$^{+/LSL\text{-}R482Q}$ mice have been previously reported [37]. All animal experiments were performed according to local ethical and UK Home Office guidelines, under regulatory approval. Haematoxylin and Eosin (H&E) staining of paraffin-embedded sections was performed as described [34]. PCR genotyping of BRAF^{V600E} floxed and Cre-recombined alleles was performed using methods and primers described in [34] and detection of the Cre-recombined allele for the *Fbxw7*^{R482Q} alleles using PCR is described in Davis et al. 2011 [37]. MEFs were derived by timed matings between relevant mouse strains and embryos were harvested at embryonic day 14.5 as described [38].

2.2. Cell culture and treatments

MEFs were cultured in DMEM with 10% (*v*/v) Foetal Calf Serum (FCS) and 1% (*v*/v) penicillin and streptomycin (P-S) at 10% CO_2. They were plated at a density of $2x10^5$ cells/well of a 6-well dish and infected with 4×10^7 PFU of Adenoviral Cre (AdCre) for 2 h in 2 ml of media lacking FCS and P-S. Media was replaced and cells were cultured for up to 96 h. For MEK inhibition, 1 μM PD184352 in DMSO was added 48 or 72 h after AdCre infection. In both cases, cells were harvested 24 h after PD184352 addition. For proteasome inhibition, 30 μM MG132 in DMSO or 0.5 μM Epoxomicin in DMSO were added for the last 5 h before harvesting. HEK293^T cells were cultured in MEF media and transfected with 5 μg plasmid using Lipofectamine 2000 in accordance with the manufacturer's instructions (Invitrogen). Cells were incubated for 48 h before harvesting. NIH3T3 cells were cultured as for MEFs and transfected with expression vectors using Lipofectamine 2000. Human cancer cell lines were grown in MEF media and treated with or without 1 μM PD184352 in DMSO for 6–48 h before harvesting.

2.3. Western blot analysis

Cells and lung tissue were lysed with gold lysis buffer (GLB) as described previously [39]. The soluble fraction (SF) was obtained by taking the supernatant following centrifugation at 13,000 rpm for 10 min at 4 °C. The insoluble fraction (IF) was obtained by treating the pellets with 1× Sample Buffer (0.05 mM Tris pH 6.8, 2% (*v*/v) SDS, 0.1% Glycerol), vortexing for 1 min and subsequently boiling for 5 min at 95 °C. Protein concentrations were measured by the Bradford assay (SF) or BCA protein assay kit (IF), both obtained from Pierce and following the manufacturer's guidelines. The following antibodies were used for analysis: BRAF (Santa Cruz 5284), ERK2 (Santa Cruz SC154), Phospho-ERK1/2 (Cell Signalling 9101), Phospho-MEK1/2 (Cell Signalling 9154S), GAPDH (EMD Millipore MAB374), β-ACTIN (Sigma S-A2103), MYC-TAG (Santa Cruz SC40), GFP (ABcam AB6556) and FLAG (Sigma F3165).

2.4. Plasmids and site-directed mutagenesis

Plasmids used for half-life experiments were either the pEF Myc-tagged BRAF^{WT} or pEF Myc-tagged BRAF^{V600E} expression vectors as previously described [3]. Site directed mutagenesis was performed using the Gene Tailor site-directed mutagenesis system (Invitrogen). For co-immunoprecipitations, vectors expressing GFP-BRAF^{WT}, GFP-BRAF^{V600E} or empty GFP vector were used together with vectors expressing ^{WT}FBXW7 or ^{R482Q}FBXW7.

2.5. Immunoprecipitations

HEK293^T cells were transfected with the appropriate plasmid vectors and GLB soluble protein lysates were generated. For GFP vectors, 200 μg protein lysate was incubated with 20 μl GFP-TRAP beads (Chromotek) in a volume of 500 μl with GLB lysis buffer rotating at 4 °C overnight. For Myc-tagged vectors, 200 μg protein lysate was incubated with 15 μl of the 9E10 antibody (200 μg/ml; Santa Cruz SC40) together with 25 μl of Dynabeads protein G (Life Technologies) in a volume of 500 μl with GLB lysis buffer rotating at 4 °C overnight. Immunoprecipitated proteins were washed three times in GLB lysis buffer before resuspension in Laemmli buffer and boiling at 95 °C for 5 min.

2.6. Pulse–chase experiments

HEK293^T cells were transiently transfected with relevant vectors as above in triplicate. 48 h after transfection cells were washed twice with sterile PBS and cultured in 3 ml of Met/Cys-free Dulbecco's modified Eagle's medium (Invitrogen) supplemented with 2 mM L-glutamine (Sigma) and 5% (*v*/v) dialysed FCS (Invitrogen) for 1 h at 37 °C. The cells were labelled with 50 μl of EXPRE^{35}S^{35}S protein labelling mixture (100 μCi/dish; PerkinElmer Life Sciences) for 3 h at 37 °C. After extensive washing, chase was initiated by adding 3 ml of MEF media to each dish and cells were lysed at appropriate time points in 500 μl of cold radioimmune precipitation assay buffer (20 mM Tris pH 7.5, 150 mM NaCl, 2 mM EDTA, 10% (*v*/v) glycerol, 1% (*v*/v) NP40, 1 mM phenylmethylsulfonyl fluoride, 1 mM NaV_3O_4, and 1 mM NaF). The samples were left on ice for 30 min to allow complete lysis, and then

centrifuged at 13,000 rpm at 4 °C for 10 min. Supernatants were collected and protein levels quantitated using the Bradford assay (Pierce). Samples were subjected to immunoprecipitation as described above, followed by SDS-PAGE. Gels were fixed in 50% (v/v) methanol and 10% (v/v) acetic acid for 30 min, washed with water several times, dried under vacuum and then exposed to a phosphoimager screen overnight. For the MEK inhibitor experiments, 1 μM PD184352 or DMSO carrier control was added at the beginning of the chase and retained in the culture media throughout the time-course.

2.7. Gel and blot quantitations

For Western blots, Image J software was used to quantitate protein levels. The background on the blots was first subtracted from the pixel counts for each band and final values were divided by the values obtained for loading controls. The control samples were set at 1.0 and all other samples were calibrated accordingly into Arbitrary Units (AU). For half-life determination, the intensity of each individual band was quantitated using the phosphoimager Quant programme (GE HealthCare). The half-life was determined to be the point at which 50% of the protein remained relative to that at t = 0.

2.8. Quantitative RT-PCR

Total RNA was extracted from MEFs using the RNeasy Mini Kit (Qiagen) and 0.5 μg RNA was reverse-transcribed using Superscript III (Invitrogen) according to the manufacturer's instructions. Quantitative RT-PCR was performed as described [40] using SYBRGreen (BioRad) in a LightCycler® 480 Real-Time PCR (Roche). Primers used were: *Gapdh* For: 5′-AGG TCG GTG TGA ACG GAT TTG-3′ and Rev: 5′-TGT AGA CCA TGT AGT TGA GGT CA-3′; *Braf* For: 5′-GAA TGT GAC AGC ACC CAC AC-3′ and Rev: 5′-ATA AGC TGG AGC CCT CAC - 3′.

2.9. Statistical analysis

Comparison between any two groups was performed by the student's *t* test. *P* values of <0.05 were considered statistically significant.

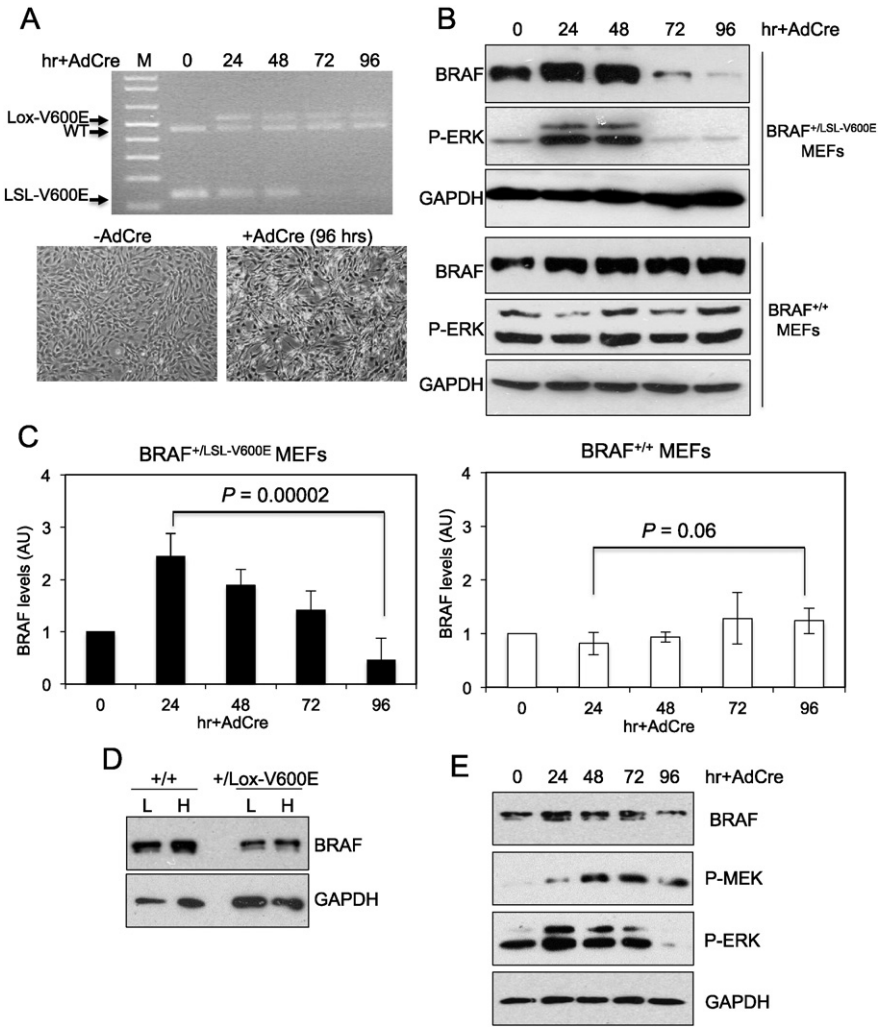

Fig. 1. Downregulation of BRAF protein levels following ^{V600E}BRAF expression in MEFs. (A) Detection of LSL and Lox alleles by PCR. Primary MEFs with the *Braf*$^{+/LSL\text{-}V600E}$ genotype were infected with AdCre for up to 96 h, DNA was isolated and PCR assays undertaken to identify LSL and Lox alleles. The photographs show the morphology of *Braf*$^{+/LSL\text{-}V600E}$ MEFs with and without AdCre for 96 h. (B) Drop in BRAF protein levels following BRAF^{V600E} expression. Soluble protein lysates were generated from *Braf*$^{+/+}$ and *Braf*$^{+/LSL\text{-}V600E}$ MEFs at the time points indicated following AdCre treatment. Protein lysates were analysed by immunoblot for BRAF and phosphoERK with GAPDH as a loading control. Representative immunoblots for four independent experiments are shown. (C) BRAF protein quantitation. BRAF protein levels were quantitated using Image J analysis of Western blot signals. The control samples were set at 1.0 and all other samples were calibrated accordingly into Arbitrary Units (AU). Data represent mean ± SD of four experiments of four independent MEFs for *Braf*$^{+/LSL\text{-}V600E}$ MEFs and three experiments of three independent MEFs for *Braf*$^{+/+}$ MEFs. (D) BRAF expression level is not affected by cell density. Soluble protein lysates were generated from *Braf*$^{+/+}$ and *Braf*$^{+/LSL\text{-}V600E}$ that had been treated with AdCre for 96 h and plated at high (H) or low (L) density. Protein lysates were analysed by immunoblot for BRAF and GAPDH was used as a loading control. (E) Analysis of phosphoMEK and phosphoERK. Soluble protein lysates were generated from *Braf*$^{+/LSL\text{-}V600E}$ MEFs at the time points indicated following AdCre treatment. Protein lysates were analysed by immunoblot for BRAF, phosphoMEK, phosphoERK with GAPDH as a loading control.

3. Results

3.1. Expression of ^{V600E}BRAF down-regulates BRAF protein levels

We have previously generated conditional knockin *Braf*$^{+/LSL\text{-}V600E}$ mice that allow expression of the oncogenic ^{V600E}BRAF protein from one allele of the endogenous *Braf* gene following Cre-mediated recombination [34]. MEFs were derived from these mice and AdCre delivered to the cells *ex vivo*. Following AdCre treatment, recombination of the LSL allele was induced, generating the Lox-V600E allele with virtual 100% recombination at 96 h post-Cre treatment (Fig. 1A). The cells were morphologically transformed following ^{V600E}BRAF expression (Fig. 1A).

The levels of expression of the BRAF protein were monitored by immunoblot analysis (Fig. 1B) and quantitation (Fig. 1C) in both *Braf*$^{+/LSL\text{-}V600E}$ and *Braf*$^{+/+}$ MEFs following AdCre treatment. Due to the presence of polyadenylation sequences within the LSL cassette, the *Braf*$^{LSL\text{-}V600E}$ allele is known to generate a hypomorphic *Braf* allele that expresses the BRAF protein at <10% the level of the wild-type *Braf* allele (Fig. 1B). Thus, following removal of the LSL cassette, BRAF protein levels within the *Braf*$^{+/LSL\text{-}V600E}$ cells are increased at 24 h following AdCre delivery (Fig. 1B and C). However, at subsequent time points (72–96 h), there was a significant decrease in BRAF protein levels (Fig. 1B and C). Such alterations in the levels of BRAF protein were not observed in *Braf*$^{+/+}$ cells following a time course of AdCre treatment, suggesting they occur as a consequence of ^{V600E}BRAF expression (Fig. 1B and C). This effect was not related to cell density as indicated by the observation that BRAF levels do not change in high or low-density cultures of *Braf*$^{+/+}$ and *Braf*$^{+/Lox\text{-}V600E}$ cells (Fig. 1D). The fact that BRAF levels drops by more than 50% in the *Braf*$^{+/LSL\text{-}V600E}$ cells would suggest that both ^{WT}BRAF and ^{V600E}BRAF proteins are affected as a consequence of expression of the oncogene.

The initial expression of ^{V600E}BRAF was accompanied by induction of phosphorylated MEK/ERK at 24–48 h post-AdCre treatment (Fig. 1B and

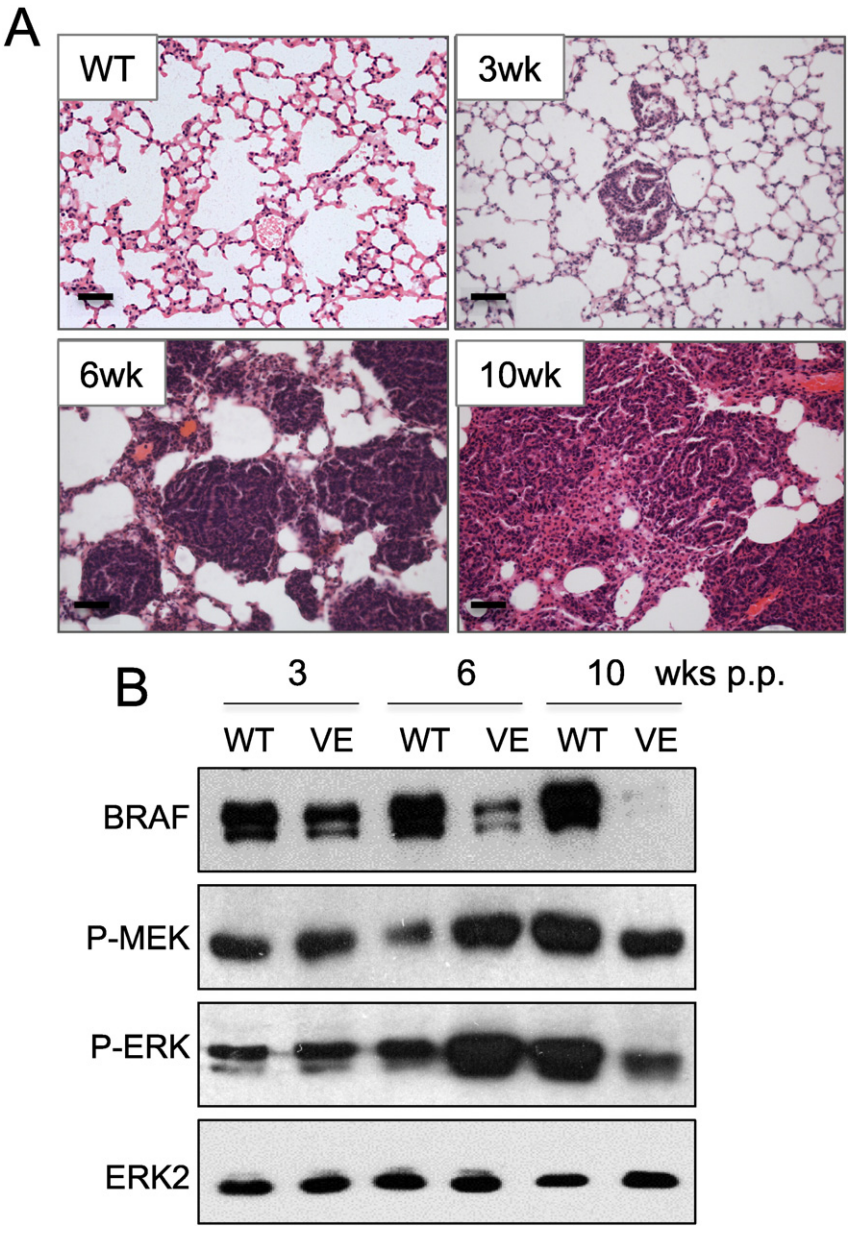

Fig. 2. Downregulation of BRAF protein levels following ^{V600E}BRAF expression in the lung. (A) Histological staining of lung tissue with H&E. Lung sections from *Braf*$^{+/+}$; *CreER*^{TM} mice at 10 weeks of age and *Braf*$^{+/LSL\text{-}V600E}$; *CreER*^{TM} mice at 3, 6 and 10 weeks of age were generated and representative H&E stained images are shown. Scale bars, 100 μm. These mice have been previously reported in [36]. (B) Drop in BRAF protein levels following BRAF^{V600E} expression. Soluble protein lysates were generated from the lungs of *Braf*$^{+/+}$; *CreER*^{TM} (WT) and *Braf*$^{+/LSL\text{-}V600E}$; *CreER*^{TM} (VE) mice at the ages shown using GLB lysis. Representative immunoblot analysis of protein lysates for BRAF, phosphoMEK and phosphoERK are shown. ERK2 was used as a loading control.

E). However, at later time points, when BRAF levels were observed to drop, there was a noticeable decrease in phosphorylated MEK/ERK (Fig. 1B and E). This result suggests that the drop in BRAF expression leads to downregulation in signalling through the MEK/ERK pathway.

To investigate whether similar responses occur *in vivo*, we assessed BRAF protein levels in lung tissue derived from *Braf*$^{+/LSL\text{-}V600E}$;*CreER*^{TM} mice that develop lung adenomas at 3–10 weeks post-partum [36] (Fig. 2A). As with the MEFs, BRAF protein levels were found to progressively decrease in the ^{V600E}BRAF-expressing lung and this was accompanied by a decrease in phosphorylated MEK and ERK levels at the 10-week time points (Fig. 2B).

3.2. The decrease in BRAF protein level is associated with alterations in protein stability

We quantitated *Braf* mRNA across the time course using qRT-PCR. *Braf* mRNA levels were decreased in both *Braf*$^{+/+}$ and *Braf*$^{+/LSL\text{-}V600E}$ cells at 24–72 h post-AdCre treatment, suggesting this is a response to the presence of Cre (Fig. 3A). However, at the 96 h time point, when BRAF protein levels are most markedly decreased in the *Braf*$^{+/LSL\text{-}V600E}$ cells (Fig. 1B, C and E), there was no significant difference between the expression of *Braf* mRNA in the *Braf*$^{+/+}$ and *Braf*$^{+/LSL\text{-}V600E}$ MEFs (Fig. 3A). This would suggest that the difference in protein expression is not underpinned by transcriptional alterations in the *Braf* gene or mRNA stability.

To investigate protein stability, the *Braf*$^{+/+}$ and *Braf*$^{+/LSL\text{-}V600E}$ MEFs at 96 h post-AdCre treatment were exposed to proteasomal inhibitors MG132 and epoxomicin. For these experiments, soluble and insoluble protein lysates were generated and analysed since proteasomal inhibition is known to lead to the accumulation of ubiquitylated proteins predominantly in detergent-insoluble fractions. Treatment with both inhibitors led to an accumulation of BRAF protein levels in soluble and insoluble fractions in both cell types (Fig. 3B). Indeed this treatment raised BRAF protein levels in the AdCre-treated *Braf*$^{+/LSL\text{-}V600E}$ cells to those similar to levels in AdCre-treated *Braf*$^{+/+}$ cells without inhibitor (Fig. 3B).

We also investigated the half-lives of ^{WT}BRAF and ^{V600E}BRAF by transfecting vectors expressing MYC-tagged versions of either of the proteins into HEK293^{T} cells and using pulse–chase analysis. As shown in Fig. 3C, ectopic ^{V600E}BRAF demonstrated a significantly shorter half-life than ectopic ^{WT}BRAF by ~3 h.

3.3. The decrease in BRAF protein level is associated with MEK activity

The fact that BRAF protein levels drop in the AdCre-treated *Braf*$^{+/LSL\text{-}V600E}$ MEFs (Fig. 1C) suggests that both ^{WT}BRAF and ^{V600E}BRAF proteins are affected by the presence of the oncogene and therefore that a downstream event is involved in this regulation. To examine a role of the MEK/ERK pathway, we treated *Braf*$^{+/LSL\text{-}V600E}$ MEFs with the MEK inhibitor PD184352 and found that this increased BRAF protein levels in both insoluble and soluble protein fractions compared to controls (Fig. 4A). Furthermore, treatment with PD184352 rescued the half-life of ^{V600E}BRAF to levels similar to ^{WT}BRAF in HEK293^{T} cells (Fig. 4B). Thus, the increased instability of the BRAF protein following ^{V600E}BRAF expression can be explained by ERK feedback regulation.

3.4. Association of feedback pathway with Oncogene-induced Senescence (OIS)

^{V600E}BRAF expression in primary mouse and human cells is known to be associated with OIS [41–45]. To investigate whether the feedback pathway identified here is associated with OIS, we analysed the ^{V600E}BRAF-expressing MEFs and HEK293^{T} cells by immunoblot with a range of senescence markers (Fig. S1). Although the HEK293^{T} cells only demonstrated weak OIS marker expression, the MEFs demonstrated induction of p21^{CIP1} and p19^{ARF} expression at the late time points. Similarly, we have previously demonstrated expression of senescence markers (p21^{CIP1} and γH2AX) in the lung tissue analysed in Fig. 2 at the 10 week time point [36] when BRAF levels are observed to drop (Fig. 2B).

To further confirm an association with OIS, we investigated whether the feedback pathway is operational in advanced, highly proliferative human cancer samples with long-term *^{V600E}BRAF* mutation acquisition. To this end, three human cancer cell lines Colo205, HT29 (both from colorectal cancers) and A375 (from a melanoma) bearing the *^{V600E}BRAF*

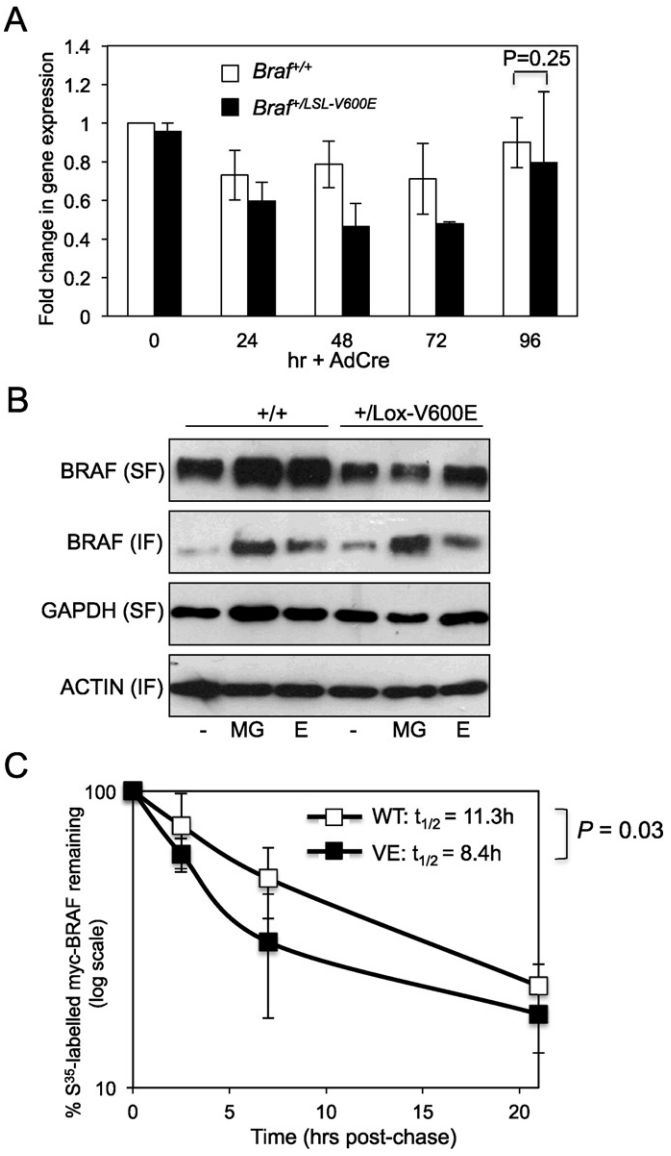

Fig. 3. Differences in BRAF protein levels are attributable to alterations in protein stability. (A) Assessment of *Braf* mRNA levels. Quantitative RT-PCR (qRT-PCR) analysis was used to investigate *Braf* mRNA levels in *Braf*$^{+/LSL\text{-}V600E}$ and *Braf*$^{+/+}$ MEFs following a time course of AdCre treatment. The graph shows the fold increase or decrease in *Braf* mRNA levels relative to the levels in the *Braf*$^{+/+}$ samples without AdCre (t = 0). Data represent mean ± SD of three independent experiments of three independent MEFs of each genotype. (B) Rescue of BRAF protein levels by proteasome inhibitors. Representative BRAF immunoblot analysis of protein lysates derived from *Braf*$^{+/Lox\text{-}V600E}$ and *Braf*$^{+/+}$ MEFs following treatment with proteasomal inhibitors are shown. *Braf*$^{+/+}$ and *Braf*$^{+/LSL\text{-}V600E}$ MEFs were infected with AdCre for 96 h and treated either with DMSO, 30 μM MG132 in DMSO or 0.5 μM Epoxomicin in DMSO for 5 h before harvesting soluble (SF) and insoluble (IF) fractions. GAPDH and β-ACTIN were used as loading controls for the SF and IF respectively. Data are representative of three experiments. (C) Half-life determination of ^{V600E}BRAF and ^{WT}BRAF in HEK293^{T} cells. Data were obtained in triplicate for three independent experiments and the graph shows mean ± SD at each time point. The average half-life of each sample is indicated.

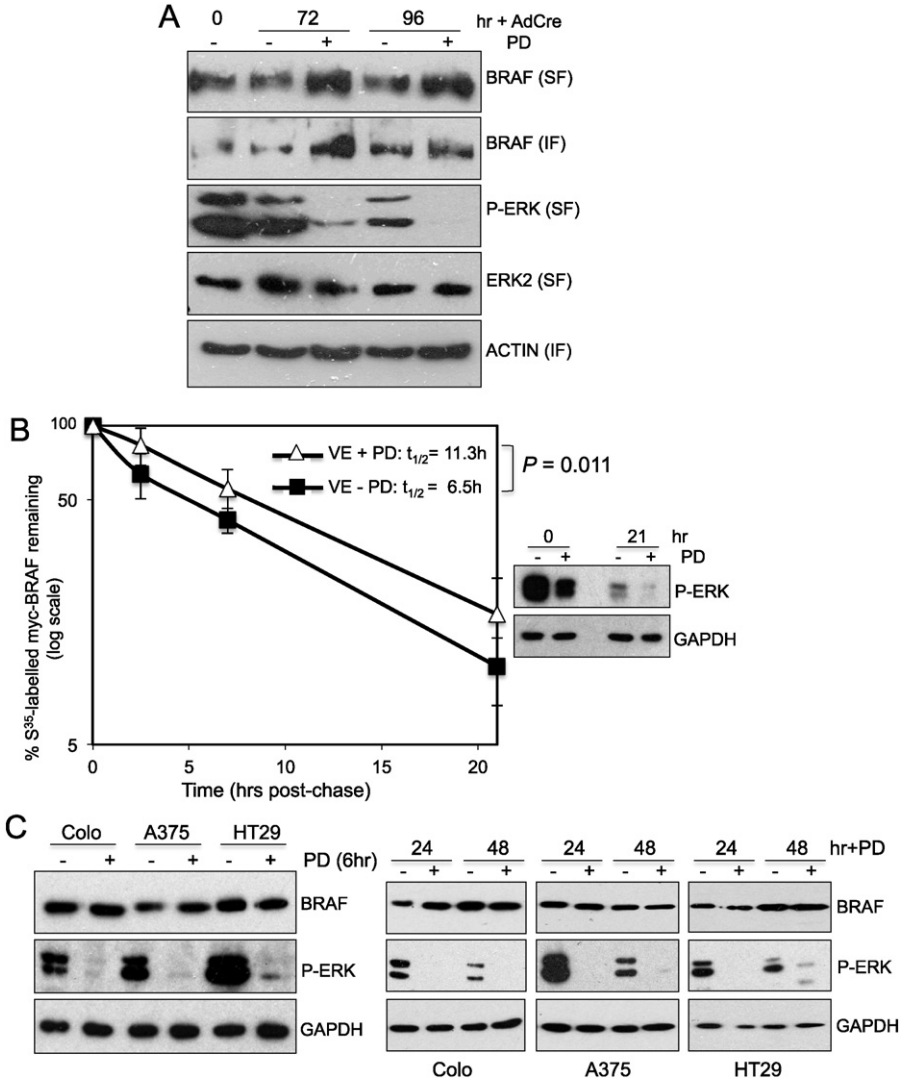

Fig. 4. BRAF protein levels are increased by MEK inhibition. (A) MEK inhibition in MEFs. Representative BRAF immunoblot analysis of protein lysates derived from SF and IF of *Braf*$^{+/LSL\text{-}V600E}$ MEFs following treatment with MEK inhibitor 1 μM PD184352 or carrier control are shown. ERK2 and β-ACTIN were used as loading controls for the SF and IF respectively. Data are representative of two experiments. (B) Half-life determination of ^{V600E}BRAF in HEK293^{T} cells following treatment with 1 μM PD184352 (+PD) or carrier control (−PD). Data were obtained in triplicate for two independent experiments and the graph shows mean ± SD at each time points. The average half-life of each treatment is indicated. (C) No alteration in BRAF levels in human cancer cell lines following MEK inhibition. Colo205, A375 and HT29 were treated with 1 μM PD184352 (+PD) or carrier control (−PD) for 6–48 h. Protein lysates were immunoblotted for BRAF and phosphoERK. GAPDH was used as a loading control. Of note, the human cancer cell lines used for this analysis do not carry mutations in *FBXW7* or known F-box containing genes (http://cancer.sanger.ac.uk/cosmic), as documented to date.

mutation were treated with PD184352 for 6–48 h and BRAF protein levels were assessed. Although this treatment resulted in a noticeably faster migrating form of BRAF, reflecting inhibition of ERK phosphorylation of BRAF [15], there were no alterations in BRAF expression levels in any of the cell lines (Fig. 4C).

3.5. BRAF stability is regulated by ERK phosphorylation sites within the CPD

Although a number of pathways controlling BRAF protein stability have been identified and reported in the literature, given the role of the ERK pathway (Fig. 4), we were particularly interested in the reported control of LIN-45 stability by MPK1 and SEL-10 (FBXW7, FBW7 or CDC4 in mammals) in *C. elegans* [33]. FBXW7 is a subunit of the SCF complex [46,47]. Substrates for SCF have a high affinity-binding site for FBXW7 within a CPD [48–50] and LIN-45 contains an ERK docking site D domain adjacent to the CPD with MPK1 capable of phosphorylating two residues (T432 and S436) within this CPD, allowing binding of FBXW7. A conserved CPD is located at residues 400–405 in human BRAF with ERK phosphorylation sites identified at residues T401 and S405 (Fig. 5A).

To investigate the role of this putative CPD in mammalian BRAF turnover, we mutated T401 and S405 to non-phosphorylatable alanine residues within Myc-tagged human ^{V600E}BRAF as single and double mutations and tested their effect on protein stability (Fig. 5B). Both of the single mutations (T401A or S405A) led to a substantial increase in the half-life of ^{V600E}BRAF compared to the non-mutated versions and the double mutation did not increase the half-life any further (Fig. 5B). This suggests that phosphorylation of both T401 and S405 is important in regulating the turnover of ^{V600E}BRAF. The half-lives of all CPD phosphorylation mutants in ^{V600E}BRAF were also increased by 4–5 h above that for ^{WT}BRAF, suggesting that disruption of the CPD may interfere with other pathways normally involved in the regulation of BRAF turnover.

To confirm that mutation of these residues within the CPD itself does not interfere with downstream signalling of ^{V600E}BRAF, we were able to show that the mutants induced ERK phosphorylation to the same levels as the non-mutated version of ^{V600E}BRAF (Fig. 5C) and they were also

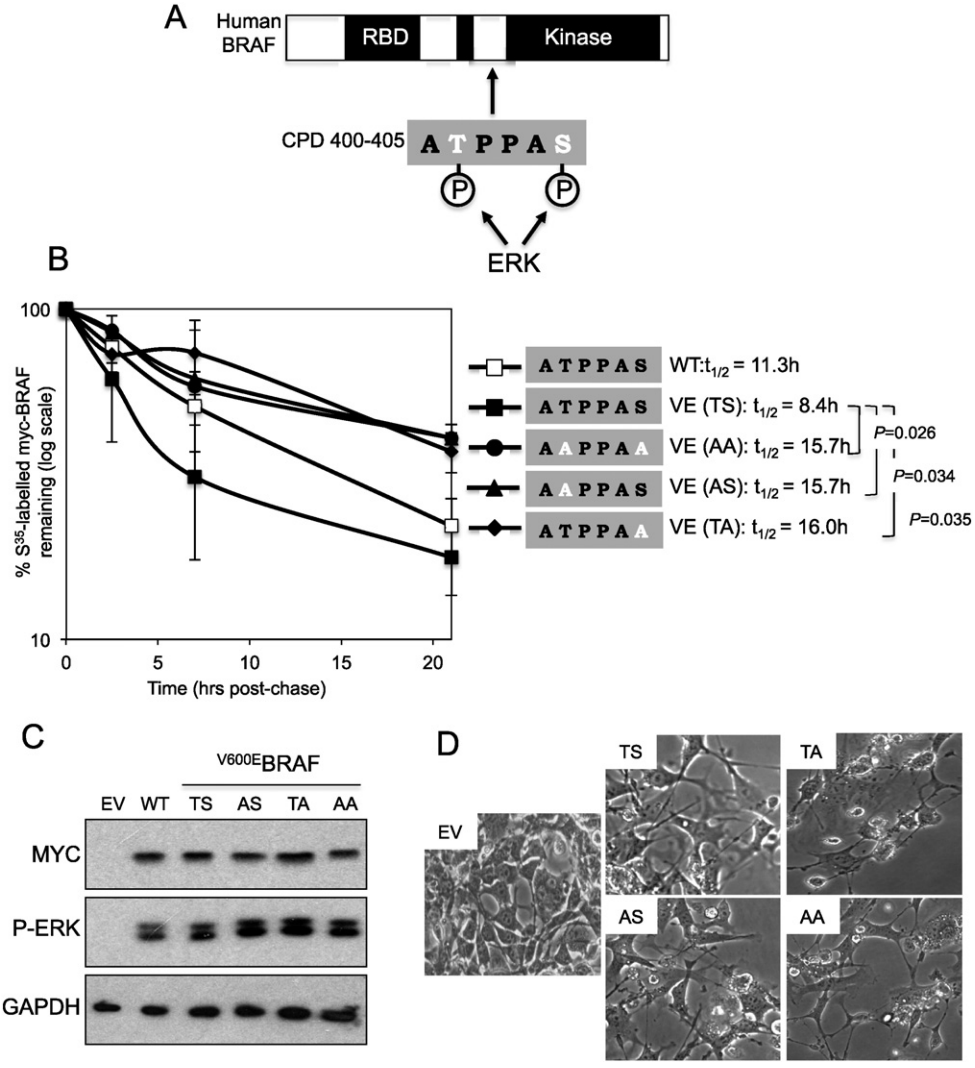

Fig. 5. BRAF turnover is regulated by ERK phosphorylation in the CPD. (A) Schematic of human BRAF to indicate potential conserved CPD at residues 400–405 and putative ERK phosphorylation sites at T401 and S405. T401 has previously been validated as a *bona-fide* ERK phosphorylation site using experimentation [15]. (B) Half-life determination of ^{V600E}BRAF, ^{WT}BRAF and ^{V600E}BRAF with CPD mutations in HEK293^{T} cells. Data were obtained in triplicate for three independent experiments and the graph shows mean ± SD at each time point. $^{TS;V600E}$BRAF represents ^{V600E}BRAF with non-mutated CPD, $^{AA;V600E}$BRAF represents ^{V600E}BRAF with the T401A;S405A double mutation in the CPD, $^{AS;V600E}$BRAF represents ^{V600E}BRAF with the T401A single mutation in the CPD and $^{TA;V600E}$BRAF represents ^{V600E}BRAF with the S405A single mutation in the CPD. The average half-life of each mutant is indicated. The data for non-CPD mutated ^{WT}BRAF and ^{V600E}BRAF are the same as that shown in Fig. 3C. (C) Immunoblot analysis of phosphoERK and MYC in protein lysates derived from HEK293^{T} cells transfected with empty vector (EV), the MYC-tagged ^{WT}BRAF expression vector and the MYC-tagged ^{V600E}BRAF expression vector with or without CPD mutations for 48 h. GAPDH was used as a loading control. (D) Photographs of NIH3T3 cells that were transfected with empty vector (EV) or the MYC-tagged ^{V600E}BRAF vector with or without CPD mutations for 48 h.

able to induce morphological transformation of NIH3T3 cells (Fig. 5D). This result is consistent with previous data showing that the T401A mutation does not have a strong effect on BRAF transforming activity [15].

3.6. The role of FBXW7 in BRAF turnover

To investigate a role of FBXW7 in mammalian BRAF protein turnover, we first examined whether the two proteins are able to interact. HEK293^{T} cells were co-transfected with vectors expressing GFP alone, GFP-tagged ^{WT}BRAF or GFP-tagged ^{V600E}BRAF with FLAG-tagged FBXW7. Soluble protein lysates were generated, immunoprecipitated using GFP trap beads and analysed by immunoblot for FLAG (Fig. 6A). The data show co-immunoprecipitation of FBXW7 with ^{WT}BRAF and ^{V600E}BRAF but not with GFP alone (Fig. 6A).

FBXW7 is involved in the binding of a number of substrates through a C terminal interacting domain made up of WD40 repeats, and arginine residues within these repeats are important for substrate recognition [48,51]. Mutation of arginine residues at 465 and 479 within the WD40 repeats are hotspots for mutations in human cancers [50,52] and mutation of the equivalent R479 mutation in mice (R482) generates increased expression of FBXW7 target substrates KLF5 and Tgifl in the mouse lung [37]. To investigate if R482 of mouse FBXW7 is involved in the binding of BRAF we repeated the above coimmunoprecipitation experiment with ^{R482Q}FBXW7. This mutated form of FBXW7 was able to interact with BRAF in a similar manner to ^{WT}FBXW7, suggesting the interaction with BRAF is not mediated by the substrate recognition domain of FBXW7 (Fig. 6A).

We then performed over expression and loss of function studies to address the role of FBXW7 in the turnover of both ^{WT}BRAF and ^{V600E}BRAF. Using the HEK293^{T} system the half-lives of ^{WT}BRAF and ^{V600E}BRAF in the presence and absence of overexpressed FBXW7 were compared. As shown in Fig. 6B, the half-lives of both ^{WT}BRAF and ^{V600E}BRAF were not shortened by the co-overexpression of FBXW7, counteracting the view that FBXW7 is involved in promoting BRAF turnover. In fact, the half-lives of both proteins was observed to increase in the presence of over-expressed FBXW7 (although not to statistically

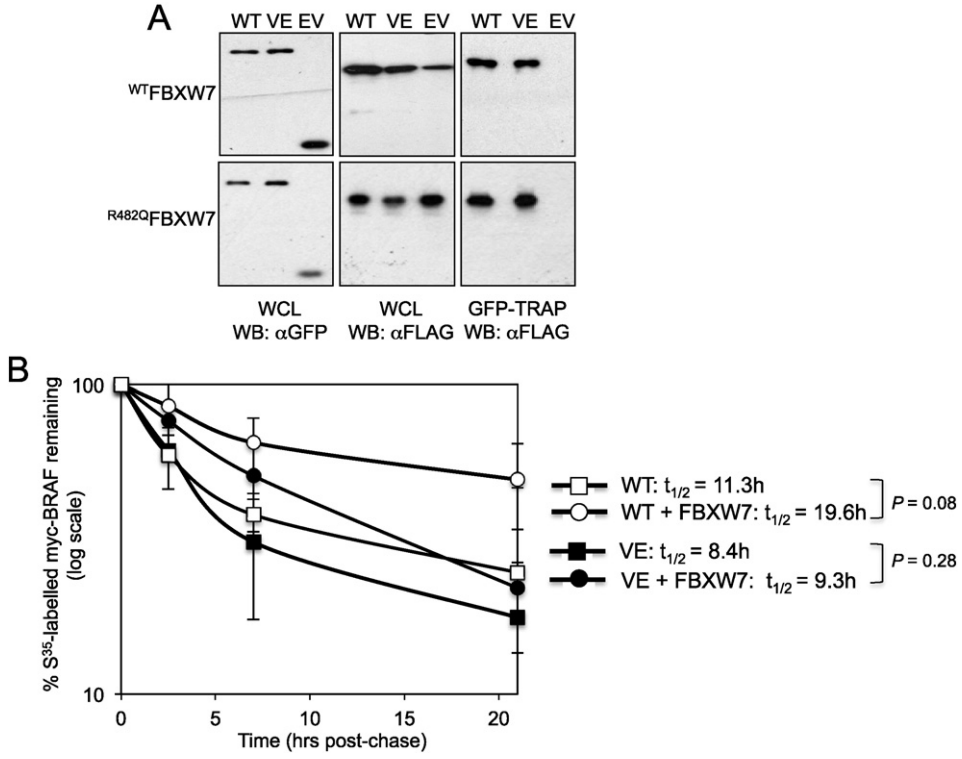

Fig. 6. FBXW7 interacts with BRAF in HEK293^{T} but does not promote BRAF turnover. (A) Co-immunoprecipitation of BRAF with wild-type and mutant FBXW7. HEK293^{T} cells were co-transfected with vectors expressing GFP-tagged ^{WT}BRAF (WT), ^{V600E}BRAF (VE) or GFP alone (EV) together with either a vector expressing FLAG-tagged ^{WT}FBXW7 (top panels) or ^{R482Q}FBXW7 (bottom panels). After 48 h, soluble protein cell lysates (WCL) were generated and these were subjected to immunoblot for GFP or FLAG. GFP-expressing proteins were immunoprecipitated using GFP-trap beads and these were subjected to immunoblot for FLAG (right panels) to examine co-immunoprecipitation of FBXW7 with BRAF. (B) Half-life determination of ^{V600E}BRAF and ^{WT}BRAF in the absence or presence of over-expressed FBXW7 in HEK293^{T} cells. HEK293^{T} cells were transfected with vectors expressing MYC-tagged ^{WT}BRAF or ^{V600E}BRAF in the presence or absence of a vector expressing FBXW7. Data were obtained in triplicate for three independent experiments and the graph shows mean ± SD at each time point. The average half-life of each condition is indicated. The data for ^{WT}BRAF and ^{V600E}BRAF are the same as that shown in Fig. 3C.

significant levels), potentially suggesting that over-expression of FBXW7 interferes with the binding of other proteins involved in regulating BRAF turnover.

To further investigate a role of FBXW7 we first attempted to undertake *Fbxw7* siRNA knockdown experiments in MEFs. However, these proved not to be successful due to the lack of specific antibodies for endogenous mouse FBXW7 (data not shown). As an alternative, we derived MEFs from mice homozygous for a floxed allele for the conditional knockin ^{R482Q}*Fbxw7* mutation [37] and examined BRAF protein expression following Cre-mediated recombination of the floxed allele. As shown in Fig. 7A, the expression level of ^{WT}BRAF was not altered following ^{R482Q}FBXW7 expression.

A similar experiment was performed with ^{V600E}BRAF in MEFs. MEFs were derived from mouse embryos containing the *Braf*$^{+/LSL\text{-}V600E}$ allele with or without the conditional homozygous knockin ^{R482Q}*Fbxw7* mutation. MEFs were treated with AdCre for 96 h, and the expression of BRAF was compared. On the ^{R482Q}*Fbxw7* mutant background, the expression level of ^{V600E}BRAF was not significantly altered compared to controls (Fig. 7B). Additionally, there were no alterations in the morphological transformation of the MEFs (Fig. 7C). These data are consistent with the view that FBXW7 does not play a unique role in regulating the turnover of ^{V600E}BRAF.

4. Discussion

Exquisite control of the RAF–MEK–ERK signalling pathway is of critical importance in the maintenance of tissue and body homeostasis and deregulation of the pathway is associated with several human pathologies including cancer, RASopathies, some neurological disorders and diabetes [53]. An understanding of the mechanisms that regulate the pathway in normal and diseased cells is imperative for the design of optimal treatments as well as for understanding drug resistance. Here we have confirmed the existence of an ERK-mediated feedback pathway controlling BRAF protein turnover in mammalian cells that was previously identified in *C. elegans* [33]. However, despite conservation of the feedback loop *via* ERK, the subsequent BRAF degradation is different in *C. elegans* and mammalian cells in that mammalian cells do not uniquely rely on the FBXW7/SEL-10 component of the SCF E3 ubiquitin ligase complex.

A variety of different methods for fine-tuning the RAF–MEK–ERK pathway have been identified in recent years, with a central point of control existing at the level of RAF, which can be controlled by both feedback and feed-forward mechanisms [9]. Regulation of RAF activity involves cycles of phosphorylation and de-phosphorylation and has become increasingly more complex with the discovery that RAF isoforms can form RAF homo/hetero dimers with different levels of kinase activity [12]. RAF is also part of a multiprotein complex, components of which can influence protein folding, stability and consequently activity [28–30]. With regard to the control of RAF protein stability, a requirement for CRAF autophosphorylation of residue S621 has been reported [40]. However, this mode of control was found not to be conserved for BRAF [40] but, instead, we have confirmed an involvement of MEK/ERK activity in the regulation of BRAF protein stability.

This regulation of BRAF protein stability by ERK extends the repertoire of feedback mechanisms by which ERK controls output of the RAF/MEK/ERK pathway. It has been previously documented that ERK1/2 can down-regulate MEK1 activity by phosphorylation of T292 and T386 [54,55], although the control of cellular MEK1 levels by ERK-dependent transcriptional methods has also been identified recently [56]. ERK control of upstream regulators has also been documented including the phosphorylation of SOS to regulate its interaction with GRB2 [57] and disruption of the CRAF–RAS interaction by phosphorylation of

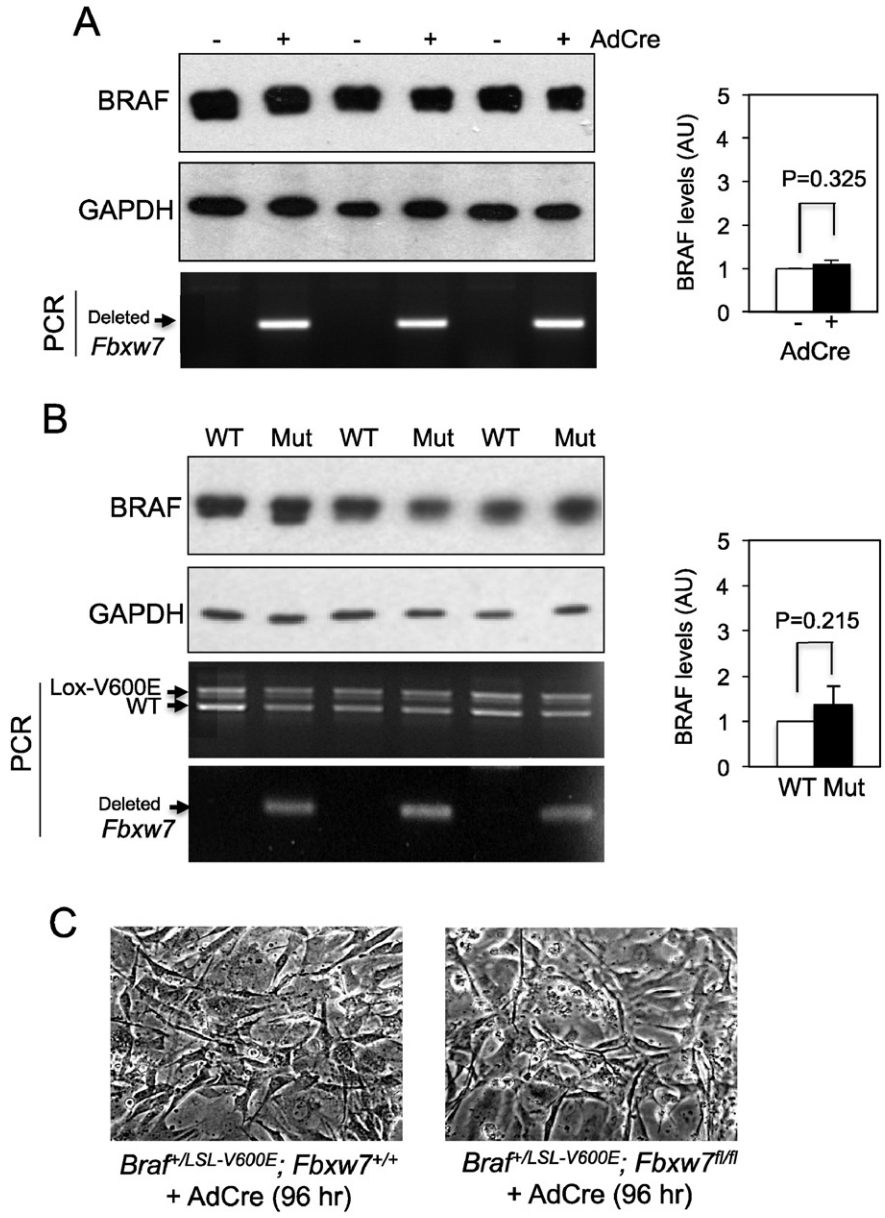

Fig. 7. Mutation of FBXW7 does not affect ^{WT}BRAF or ^{V600E}BRAF expression in MEFs. (A) Expression of ^{WT}BRAF in MEFs with the homozygous ^{R482Q}*Fbxw7* mutation. MEFs homozygous for the *Fbxw7*$^{fl/fl}$ allele were treated with or without AdCre for 96 h. Protein lysates were generated and immunoblotted for BRAF. GAPDH was used as a loading control. DNA was also generated and subjected to PCR for the Cre-deleted ^{R482Q}*Fbxw7* floxed allele. Quantitation of BRAF protein levels is shown in the bar graph on the right. Data represent mean ± SD of three independent experiments of three independent MEFs. (B) Expression of ^{V600E}BRAF in MEFs with or without the homozygous ^{R482Q}*Fbxw7* mutation. MEFs were generated from mice that contained the LSL-^{V600E}Braf genetic modification with (Mut) or without (WT) the *Fbxw7*$^{fl/fl}$ allele. MEFs were treated with AdCre for 96 h. Protein lysates were generated and immunoblotted for BRAF. GAPDH was used as a loading control. DNA was also generated and subjected to PCR for the Cre-recombined LSL-^{V600E}*Braf* allele and the Cre-deleted *Fbxw7* floxed allele. Quantitation of BRAF protein levels is shown in the bar graph on the right. Data represent mean ± SD of three independent experiments of three independent MEFs. (C) Morphology of *Braf*$^{+/LSL\text{-}V600E}$ MEFs with or without the homozygous *Fbxw7*^{R482Q} mutation treated with AdCre for 96 h.

CRAF on multiple sites [16]. With regard to BRAF, several target ERK phosphorylation sites are known to exist at S151, T401, S750 and T753 and phosphorylation of all of the sites has been shown to contribute to disruption of BRAF/CRAF heterodimerisation [12,15]. We now show that ERK phosphorylation of T401 and S405 has an additional function in controlling BRAF protein stability.

We were first drawn to investigating BRAF protein turnover by the observation that BRAF protein levels are significantly decreased in mouse cells and tissue expressing autochthonous BRAF following short term ^{V600E}BRAF expression (Figs. 1 and 2). This finding was supported by observations in the HEK293^{T} over-expression systems, demonstrating a shorter half-life of ^{V600E}BRAF than ^{WT}BRAF (Figs. 3–5). The physiological role of this feedback mechanism is presently not clear, although our data (Fig. S1) suggest a potential link with the OIS phenotype. Short-term expression of ^{V600E}BRAF is known to be associated with the induction of senescence in the mouse lung model [36,42] as well as ^{V600E}BRAF intestinal [43] and melanoma mouse models [44] and the RAF/MEK/ERK pathway is known to mediate growth inhibitory signalling as well as cell proliferation [58]. Low levels of phospho-ERK are associated with this phenotype in the mouse lung models (Fig. 2 and [59]) and, furthermore, human melanocytic naevi bearing the ^{V600E}BRAF oncogene demonstrate hallmarks of senescence [45] but <25% show detectable phospho-ERK immunohistochemical staining [60]. On this basis it has been suggested that feedback loops may be a requirement for maintenance of ^{V600E}BRAF-induced senescence [60] as has been documented for oncogenic RAS-induced senescence [61].

Further investigation of this will require manipulation of the various feedback loops associated with the RAF/MEK/ERK pathway including autochthonous mutation of ERK phosphorylation sites within the CPD and correlation with physiological responses. The fact that the ERK-mediated control of BRAF protein stability is not detected in human cancer cell lines (Fig. 4C), is consistent with a hypothesis that advanced cancers have evolved mechanisms to overcome this feedback regulation in order to bypass OIS.

FBXW7 is a member of the F-box protein family, which contain seven tandem WD40 repeats besides the F box, and is a substrate receptor component of the SCF ubiquitin ligase complex. Substrate phosphorylation within a CPD motif instigates FBXW7 binding leading to degradation of the substrate by the SCF complex [50]. Indeed, *FBXW7* mutations are associated with many human cancers and FBXW7 has been implicated as a tumour suppressor by targeting the degradation of oncoprotein substrates including Cyclin E, Notch 1 and C-Myc. Although we found that FBXW7 is capable of binding BRAF, neither the binding nor stability of BRAF was affected by the ^{R482Q}FBXW7 mutation within its WD40 substrate recognition domain (Figs. 6 and 7), the equivalent mutation of which (R479Q) is detected in many human cancers. Taken together, these results suggest that other E3 ubiquitin ligase complexes are involved in regulating BRAF turnover, the identity of which has yet to be revealed. Our data currently do not rule out a role of other components of the SCF complex or F-box proteins.

In summary, our data show that BRAF protein stability is controlled by a negative feedback loop involving ERK phosphorylation of T401 and S405 within a conserved CPD. Although this feedback pathway is activated upon short-term expression of ^{V600E}BRAF, its functional role in mediating proliferative/senescence responses are not clear and will require further investigation.

Supplementary data to this article can be found online at http://dx.doi.org/10.1016/j.cellsig.2016.02.009.

Disclosure statement

The authors declare that there are no conflicts of interests.

Acknowledgements

We thank the Division of Biomedical Services at Leicester for their invaluable support and Ian Tomlinson for providing the ^{F482Q}Fbxw7 mutant mice. This work was supported by a Conacyt Overseas Scholarship from the Mexican Consejo Nacional de Ciencia y Tecnología to MAG, a Royal Society-Wolfson Merit award 2009/R3 to CP, CRUK Programme grant A13803 and Worldwide Cancer Research project grant 08-0412.

References

[1] M. Raman, W. Chen, M.H. Cobb, Differential regulation and properties of MAPKs, Oncogene 26 (2007) 3100–3112.
[2] J.K. Osborne, E. Zaganjor, M.H. Cobb, Signal control through Raf: in sickness and in health, Cell Res. 22 (2012) 14–22.
[3] H. Davies, G.R. Bignell, C. Cox, P. Stephens, S. Edkins, S. Clegg, J. Teague, H. Woffendin, M.J. Garnett, W. Bottomley, N. Davis, E. Dicks, R. Ewing, Y. Floyd, K. Gray, S. Hall, R. Hawes, J. Hughes, V. Kosmidou, A. Menzies, C. Mould, A. Parker, C. Stevens, S. Watt, S. Hooper, R. Wilson, H. Jayatilake, B.A. Gusterson, C. Cooper, J. Shipley, D. Hargrave, K. Pritchard- Jones, N. Maitland, G. Chenevix-Trench, G.J. Riggins, D.D. Bigner, G. Palmieri, A. Cossu, A. Flanagan, A. Nicholson, J.W. Ho, S.Y. Leung, S.T. Yuen, B.L. Weber, H.F. Seigler, T.L. Darrow, H. Paterson, R. Marais, C.J. Marshall, R. Wooster, M.R. Stratton, P.A. Futreal, Mutations of the BRAF gene in human cancer, Nature 417 (2002) 949–954.
[4] C. Wellbrock, L. Ogilvie, D. Hedley, M. Karasarides, J. Martin, D. Niculescu-Duvaz, C.J. Springer, R. Marais, V599EB-RAF is an oncogene in melanocytes, Cancer Res. 64 (2004) 2338–2342.
[5] D.B. Solit, L.A. Garraway, C.A. Pratilas, A. Sawai, G. Getz, A. Basso, Q. Ye, J.M. Lobo, Y. She, I. Osman, T.R. Golub, J. Sebolt-Leopold, W.R. Sellers, N. Rosen, BRAF mutation predicts sensitivity to MEK inhibition, Nature 439 (2006) 358–362.
[6] P.T. Wan, M.J. Garnett, S.M. Roe, S. Lee, D. Niculescu-Duvaz, V.M. Good, C.M. Jones, C.J. Marshall, C.J. Springer, D. Barford, R. Marais, P. Cancer Genome, Mechanism of activation of the RAF–ERK signaling pathway by oncogenic mutations of B-RAF, Cell 116 (2004) 855–867.
[7] G. Galabova-Kovacs, D. Matzen, D. Piazzolla, K. Meissl, T. Plyushch, A.P. Chen, A. Silva, M. Baccarini, Essential role of B-raf in ERK activation during extraembryonic development, Proc. Natl. Acad. Sci. U. S. A. 103 (2006) 1325–1330.
[8] L. Wojnowski, A.M. Zimmer, T.W. Beck, H. Hahn, R. Bernal, U.R. Rapp, A. Zimmer, Endothelial apoptosis in Braf-deficient mice, Nat. Genet. 16 (1997) 293–297.
[9] R. Avraham, Y. Yarden, Feedback regulation of EGFR signalling: decision making by early and delayed loops, Nat. Rev. Mol. Cell Biol. 12 (2011) 104–117.
[10] W. Kolch, Coordinating ERK/MAPK signalling through scaffolds and inhibitors, Nat. Rev. Mol. Cell Biol. 6 (2005) 827–837.
[11] S. Torii, K. Nakayama, T. Yamamoto, E. Nishida, Regulatory mechanisms and function of ERK MAP kinases, J. Biochem. 136 (2004) 557–561.
[12] L.K. Rushworth, A.D. Hindley, E. O'Neill, W. Kolch, Regulation and role of Raf-1/B-Raf heterodimerization, Mol. Cell. Biol. 26 (2006) 2262–2272.
[13] M.J. Garnett, S. Rana, H. Paterson, D. Barford, R. Marais, Wild-type and mutant B-RAF activate C-RAF through distinct mechanisms involving heterodimerization, Mol. Cell 20 (2005) 963–969.
[14] M.A. Farrar, J. Alberol-Ila, R.M. Perlmutter, Activation of the Raf-1 kinase cascade by coumermycin-induced dimerization, Nature 383 (1996) 178–181.
[15] D.A. Ritt, D.M. Monson, S.I. Specht, D.K. Morrison, Impact of feedback phosphorylation and Raf heterodimerization on normal and mutant B-Raf signaling, Mol. Cell. Biol. 30 (2010) 806–819.
[16] M.K. Dougherty, J. Muller, D.A. Ritt, M. Zhou, X.Z. Zhou, T.D. Copeland, T.P. Conrads, T.D. Veenstra, K.P. Lu, D.K. Morrison, Regulation of Raf-1 by direct feedback phosphorylation, Mol. Cell 17 (2005) 215–224.
[17] R. Marais, Y. Light, H.F. Paterson, C.J. Marshall, Ras recruits Raf-1 to the plasma membrane for activation by tyrosine phosphorylation, EMBO J. 14 (1995) 3136–3145.
[18] H. Hanafusa, S. Torii, T. Yasunaga, E. Nishida, Sprouty1 and Sprouty2 provide a control mechanism for the Ras/MAPK signalling pathway, Nat. Cell Biol. 4 (2002) 850–858.
[19] N. Hacohen, S. Kramer, D. Sutherland, Y. Hiromi, M.A. Krasnow, Sprouty encodes a novel antagonist of FGF signaling that patterns apical branching of the *Drosophila* airways, Cell 92 (1998) 253–263.
[20] T. Wakioka, A. Sasaki, R. Kato, T. Shouda, A. Matsumoto, K. Miyoshi, M. Tsuneoka, S. Komiya, R. Baron, A. Yoshimura, Spred is a sprouty-related suppressor of Ras signalling, Nature 412 (2001) 647–651.
[21] C.J. Caunt, S.M. Keyse, Dual-specificity MAP kinase phosphatases (MKPs): shaping the outcome of MAP kinase signalling, FEBS J. 280 (2013) 489–504.
[22] P. Rodriguez-Viciana, J. Oses-Prieto, A. Burlingame, M. Fried, F. McCormick, A phosphatase holoenzyme comprised of Shoc2/Sur8 and the catalytic subunit of PP1 functions as an M-Ras effector to modulate Raf activity, Mol. Cell 22 (2006) 217–230.
[23] A.S. Dhillon, A. von Kriegsheim, J. Grindlay, W. Kolch, Phosphatase and feedback regulation of Raf-1 signaling, Cell Cycle 6 (2007) 3–7.
[24] C.A. Pratilas, B.S. Taylor, Q. Ye, A. Viale, C. Sander, D.B. Solit, N. Rosen, (V600E)BRAF is associated with disabled feedback inhibition of RAF–MEK signaling and elevated transcriptional output of the pathway, Proc. Natl. Acad. Sci. U. S. A. 106 (2009) 4519–4524.
[25] T. Murphy, S. Hori, J. Sewell, V.J. Gnanapragasam, Expression and functional role of negative signalling regulators in tumour development and progression, Int. J. Cancer 127 (2010) 2491–2499.
[26] C.A. Joazeiro, S.S. Wing, H. Huang, J.D. Leverson, T. Hunter, Y.C. Liu, The tyrosine kinase negative regulator c-Cbl as a RING-type, E2-dependent ubiquitin-protein ligase, Science 286 (1999) 309–312.
[27] K. Haglund, S. Sigismund, S. Polo, I. Szymkiewicz, P.P. Di Fiore, I. Dikic, Multiple monoubiquitination of RTKs is sufficient for their endocytosis and degradation, Nat. Cell Biol. 5 (2003) 461–466.
[28] A. Maloney, P. Workman, HSP90 as a new therapeutic target for cancer therapy: the story unfolds, Expert. Opin. Biol. Ther. 2 (2002) 3–24.
[29] S. da Rocha Dias, F. Friedlos, Y. Light, C. Springer, P. Workman, R. Marais, Activated B-RAF is an Hsp90 client protein that is targeted by the anticancer drug 17-allylamino-17-demethoxygeldanamycin, Cancer Res. 65 (2005) 10686–10691.
[30] O.M. Grbovic, A.D. Basso, A. Sawai, Q. Ye, P. Friedlander, D. Solit, N. Rosen, V600E B-Raf requires the Hsp90 chaperone for stability and is degraded in response to Hsp90 inhibitors, Proc. Natl. Acad. Sci. U. S. A. 103 (2006) 57–62.
[31] R.S. Samant, P.A. Clarke, P. Workman, E3 ubiquitin ligase Cullin-5 modulates multiple molecular and cellular responses to heat shock protein 90 inhibition in human cancer cells, Proc. Natl. Acad. Sci. U. S. A. 111 (2014) 6834–6839.
[32] S.W. Hong, D.H. Jin, J.S. Shin, J.H. Moon, Y.S. Na, K.A. Jung, S.M. Kim, J.C. Kim, K.P. Kim, Y.S. Hong, J.L. Lee, E.K. Choi, J.S. Lee, T.W. Kim, Ring finger protein 149 is an E3 ubiquitin ligase active on wild-type v-Raf murine sarcoma viral oncogene homolog B1 (BRAF), J. Biol. Chem. 287 (2012) 24017–24025.
[33] C. de la Cova, I. Greenwald, SEL-10/Fbw7-dependent negative feedback regulation of LIN-45/Braf signaling in *C. elegans* via a conserved phosphodegron, Genes Dev. 26 (2012) 2524–2535.
[34] K. Mercer, S. Giblett, S. Green, D. Lloyd, S. DaRocha Dias, M. Plumb, R. Marais, C. Pritchard, Expression of endogenous oncogenic V600EB-raf induces proliferation and developmental defects in mice and transformation of primary fibroblasts, Cancer Res. 65 (2005) 11493–11500.
[35] S. Hayashi, A.P. McMahon, Efficient recombination in diverse tissues by a tamoxifen-inducible form of Cre: a tool for temporally regulated gene activation/inactivation in the mouse, Dev. Biol. 244 (2002) 305–318.
[36] T. Kamata, H. Jin, S. Giblett, B. Patel, F. Patel, C. Foster, C. Pritchard, The cholesterol-binding protein NPC2 restrains recruitment of stromal macrophage-lineage cells to early-stage lung tumours, EMBO Mol. Med. (2015), http://dx.doi.org/10.15252/emmm.201404838.
[37] H. Davis, A. Lewis, B. Spencer-Dene, H. Tateossian, G. Stamp, A. Behrens, I. Tomlinson, FBXW7 mutations typically found in human cancers are distinct from null alleles and disrupt lung development, J. Pathol. 224 (2011) 180–189.

[38] M. Huser, J. Luckett, A. Chiloeches, K. Mercer, M. Iwobi, S. Giblett, X.M. Sun, J. Brown, R. Marais, C. Pritchard, MEK kinase activity is not necessary for Raf-1 function, EMBO J. 20 (2001) 1940–1951.
[39] J.C. Luckett, M.B. Huser, N. Giagtzoglou, J.E. Brown, C.A. Pritchard, Expression of the A-raf proto-oncogene in the normal adult and embryonic mouse, Cell Growth Differ. 11 (2000) 163–171.
[40] C. Noble, K. Mercer, J. Hussain, L. Carragher, S. Giblett, R. Hayward, C. Patterson, R. Marais, C.A. Pritchard, CRAF autophosphorylation of serine 621 is required to prevent its proteasome-mediated degradation, Mol. Cell 31 (2008) 862–872.
[41] T. Kuilman, C. Michaloglou, L.C. Vredeveld, S. Douma, R. van Doorn, C.J. Desmet, L.A. Aarden, W.J. Mooi, D.S. Peeper, Oncogene-induced senescence relayed by an interleukin-dependent inflammatory network, Cell 133 (2008) 1019–1031.
[42] D. Dankort, E. Filenova, M. Collado, M. Serrano, K. Jones, M. McMahon, A new mouse model to explore the initiation, progression, and therapy of BRAFV600E-induced lung tumors, Genes Dev. 21 (2007) 379–384.
[43] L.A. Carragher, K.R. Snell, S.M. Giblett, V.S. Aldridge, B. Patel, S.J. Cook, D.J. Winton, R. Marais, C.A. Pritchard, V600EBraf induces gastrointestinal crypt senescence and promotes tumour progression through enhanced CpG methylation of p16INK4a, EMBO Mol. Med. 2 (2010) 458–471.
[44] N. Dhomen, J.S. Reis-Filho, S. da Rocha Dias, R. Hayward, K. Savage, V. Delmas, L. Larue, C. Pritchard, R. Marais, Oncogenic Braf induces melanocyte senescence and melanoma in mice, Cancer Cell 15 (2009) 294–303.
[45] C. Michaloglou, L.C. Vredeveld, M.S. Soengas, C. Denoyelle, T. Kuilman, C.M. van der Horst, D.M. Majoor, J.W. Shay, W.J. Mooi, D.S. Peeper, BRAFE600-associated senescence-like cell cycle arrest of human naevi, Nature 436 (2005) 720–724.
[46] R.M. Feldman, C.C. Correll, K.B. Kaplan, R.J. Deshaies, A complex of Cdc4p, Skp1p, and Cdc53p/cullin catalyzes ubiquitination of the phosphorylated CDK inhibitor Sic1p, Cell 91 (1997) 221–230.
[47] D. Skowyra, K.L. Craig, M. Tyers, S.J. Elledge, J.W. Harper, F-box proteins are receptors that recruit phosphorylated substrates to the SCF ubiquitin-ligase complex, Cell 91 (1997) 209–219.
[48] M. Welcker, B.E. Clurman, FBW7 ubiquitin ligase: a tumour suppressor at the crossroads of cell division, growth and differentiation, Nat. Rev. Cancer 8 (2008) 83–93.
[49] P. Nash, X. Tang, S. Orlicky, Q. Chen, F.B. Gertler, M.D. Mendenhall, F. Sicheri, T. Pawson, M. Tyers, Multisite phosphorylation of a CDK inhibitor sets a threshold for the onset of DNA replication, Nature 414 (2001) 514–521.
[50] R.J. Davis, M. Welcker, B.E. Clurman, Tumor suppression by the Fbw7 ubiquitin ligase: mechanisms and opportunities, Cancer Cell 26 (2014) 455–464.
[51] B. Hao, S. Oehlmann, M.E. Sowa, J.W. Harper, N.P. Pavletich, Structure of a Fbw7-Skp1-cyclin E complex: multisite-phosphorylated substrate recognition by SCF ubiquitin ligases, Mol. Cell 26 (2007) 131–143.
[52] S. Akhoondi, D. Sun, N. von der Lehr, S. Apostolidou, K. Klotz, A. Maljukova, D. Cepeda, H. Fiegl, D. Dafou, C. Marth, E. Mueller-Holzner, M. Corcoran, M. Dagnell, S.Z. Nejad, B.N. Nayer, M.R. Zali, J. Hansson, S. Egyhazi, F. Petersson, P. Sangfelt, H. Nordgren, D. Grander, S.I. Reed, M. Widschwendter, O. Sangfelt, C. Spruck, FBXW7/hCDC4 is a general tumor suppressor in human cancer, Cancer Res. 67 (2007) 9006–9012.
[53] E.K. Kim, E.J. Choi, Pathological roles of MAPK signaling pathways in human diseases, Biochim. Biophys. Acta 1802 (2010) 396–405.
[54] A. Brunet, G. Pages, J. Pouyssegur, Growth factor-stimulated MAP kinase induces rapid retrophosphorylation and inhibition of MAP kinase kinase (MEK1), FEBS Lett. 346 (1994) 299–303.
[55] S.T. Eblen, J.K. Slack-Davis, A. Tarcsafalvi, J.T. Parsons, M.J. Weber, A.D. Catling, Mitogen-activated protein kinase feedback phosphorylation regulates MEK1 complex formation and activation during cellular adhesion, Mol. Cell. Biol. 24 (2004) 2308–2317.
[56] S.K. Hong, P.K. Wu, M. Karkhanis, J.I. Park, ERK1/2 can feedback-regulate cellular MEK1/2 levels, Cell. Signal. 27 (2015) 1939–1948.
[57] S. Corbalan-Garcia, S.S. Yang, K.R. Degenhardt, D. Bar-Sagi, Identification of the mitogen-activated protein kinase phosphorylation sites on human Sos1 that regulate interaction with Grb2, Mol. Cell. Biol. 16 (1996) 5674–5682.
[58] D. Woods, D. Parry, H. Cherwinski, E. Bosch, E. Lees, M. McMahon, Raf-induced proliferation or cell cycle arrest is determined by the level of rRaf activity with arrest mediated by p21Cip1, Mol. Cell. Biol. 17 (1997) 5598–5611.
[59] C.L. Trejo, J. Juan, S. Vicent, A. Sweet-Cordero, M. McMahon, MEK1/2 inhibition elicits regression of autochthonous lung tumors induced by KRASG12D or BRAFV600E, Cancer Res. 72 (2012) 3048–3059.
[60] C. Michaloglou, L.C. Vredeveld, W.J. Mooi, D.S. Peeper, BRAF(E600) in benign and malignant human tumours, Oncogene 27 (2008) 877–895.
[61] S. Courtois-Cox, S.M. Genther Williams, E.E. Reczek, B.W. Johnson, L.T. McGillicuddy, C.M. Johannessen, P.E. Hollstein, M. MacCollin, K. Cichowski, A negative feedback signaling network underlies oncogene-induced senescence, Cancer Cell 10 (2006) 459–472.